Journal of Luminescence 275 (2024) 120756

Contents lists available at ScienceDirect

Journal of Luminescence

journal homepage: www.elsevier.com/locate/jlumin

Full Length Article

Atomic-like UV emission generated in hexagonal boron nitride single crystals by thermal annealing

N. Maharjan [a], P. Joshi [b], E. Janzen [c], J.H. Edgar [c], N. Khan [d], M.L. Nakarmi [a,*]

[a] Department of Physics, Brooklyn College and the Graduate Center of the City University of New York, Brooklyn, NY, 11210, USA
[b] Physics Department, Bhaktapur Multiple Campus, Tribhuvan University, Nepal
[c] Tim Taylor Department of Chemical Engineering, Kansas State University, Manhattan, KS, 66506, USA
[d] George Gwinnett College, School of Science and Technology, Lawrenceville, GA, 30043, USA

ARTICLE INFO

Keywords:
Hexagonal boron nitride (h-BN)
Atomic-like emission
Deep UV photoluminescence (PL)

ABSTRACT

A series of atomic-like photoluminescence (PL) emission peaks in UV region near 4.0 eV were created by thermal annealing hexagonal boron nitride (h-BN) single crystals in air. The pristine h-BN did not have these peaks, emitting strong phonon-assisted band edge PL with peaks at 5.78 and 5.89 eV. After annealing the h-BN crystals in ambient air, a new atomic-like sharp emission in UV region at 4.09 eV with a line width of 0.2 nm appeared along with its phonon replicas at 3.89 and 3.69 eV in the low temperature (8 K) PL measurement. Further testing demonstrated that annealing the h-BN samples in the temperature window of 700–950 °C for 60 min generated the atomic-like emission. The peak position of the emission line is stable with the temperature and PL excitation power. Our study also suggests that the defect responsible for the atomic-like emission resides in the surface region.

1. Introduction

For many years, hexagonal boron nitride (h-BN) has been used as a chemically and thermally stable, electrically insulating, and thermal conducting ceramic [1]. Since lasing was demonstrated at wavelength (λ) ~ 215 nm by electron beam excitation from a bulk h-BN crystal in 2004, it has attracted interest for its potential in the deep ultraviolet (UV) photonics [2]. Due to its bright luminescence in the deep UV, h-BN was previously believed to be a direct bandgap material. However, based on photoluminescence (PL) experiments with two-photon excitation, Cassabois et al. [3], proved that h-BN is an indirect bandgap semiconductor with energy bandgap ~ 6 eV with a valence band maximum and conduction band minimum at the K and M points of the first Brillouin zone, respectively. Despite its indirect bandgap, its deep UV band-edge emissions produced via phonon-assisted electronic transitions have potential applications as a UV emitter for general purpose lighting, surface disinfection, and sterilization [4,5]. There is a huge demand of portable deep UV light sources in germicidal range ($\lambda < 280$ nm) for disinfection after the Covid-19 pandemic. Deep UV light sources from h-BN could be used as efficient luminescent sources/sensors [6,7]. h-BN based devices are promising for solid state neutron detectors and cameras for detecting fissile material and medical imaging [8]. Because of its layered crystal structure and wide energy bandgap, h-BN monolayer is an interesting 2D material [9]. Due to their similar crystal structures, graphene and h-BN heterostructures have been widely studied [10,11].

Recently, h-BN has also emerged as a promising candidate for single photon sources [12]. Single photon emissions from h-BN have been reported by many groups in the infrared and visible spectral regions from the samples prepared by different methods [13–18]. The most widely reported emissions are peak positions of 1.57, 1.9, 2.24 and 2.6 eV. Single photon emission from h-BN was also reported in UV region at 4.1 eV using cathodoluminescence [19]. Highly localized defect-states in wide bandgap materials behave as atomic scale electronic states and the electronic transitions in such states produce atomic-like sharp emissions. Emission from a single point defect from such material is a source of single photon emitter. Although the 4.1 eV emission line was also observed from h-BN bulk crystals, powders, and thin films, its cause is still unclear [20–23]. Documenting its optical properties and cause is important for identifying its chemical structure and for developing its application in practical devices. In this paper, we report that thermal annealing creates an atomic-like sharp emission at 4.09 eV in h-BN single crystal flakes grown by nickel-chromium (Ni–Cr) flux method. We investigated the annealing conditions needed to generate the

* Corresponding author.
E-mail address: mlnakarmi@brooklyn.cuny.edu (M.L. Nakarmi).

https://doi.org/10.1016/j.jlumin.2024.120756
Received 22 April 2024; Received in revised form 7 June 2024; Accepted 17 June 2024
Available online 22 June 2024
0022-2313/Published by Elsevier B.V.

atomic-like UV emission. Annealing the h-BN crystals in the temperature window of 700–950 °C for 60 min in ambient air proved successful. For further insights, we will also present the optical properties of the emission line from the temperature and power dependent PL measurements.

2. Experiment

The samples investigated in this study are single crystal h-BN flakes grown by the nickel-chromium (Ni–Cr) flux method [24,25]. The optical properties of the h-BN were characterized by deep UV photoluminescence spectroscopy. The PL system consists of a Coherent ultrafast Ti-Sapphire laser (pulse width ~100 fs, frequency: 76 MHz) coupled with a third harmonic generator (THG) and then a fourth harmonic generator (FHG) to generate harmonic wavelengths at 266 and 200 nm with average powers of around 100 and 2 mW, respectively. The fourth harmonic laser output was used for above bandgap photoexcitation of the h-BN samples in the PL measurements. The detection system has a Princeton 750 mm monochromator with extreme UV blazed grating and a photomultiplier tube. For the low temperature and temperature dependent measurements, we used a Janis closed-cycle cryostat along with Lakeshore temperature controller that can vary the temperature from 8 to 300 K. The laser power density was varied with neutral density filters.

We first performed the PL measurements of an unannealed h-BN sample. To investigate the effect of annealing on the optical properties, flakes of h-BN single crystal samples from the same batch of crystal growth were put on a silicon handle substrate and annealed in ambient air. The effects of annealing temperature and time were investigated. The annealing temperature was changed from 300 to 1000 °C, and time was varied from 20 to 60 min. All the h-BN samples were characterized by the deep UV PL system.

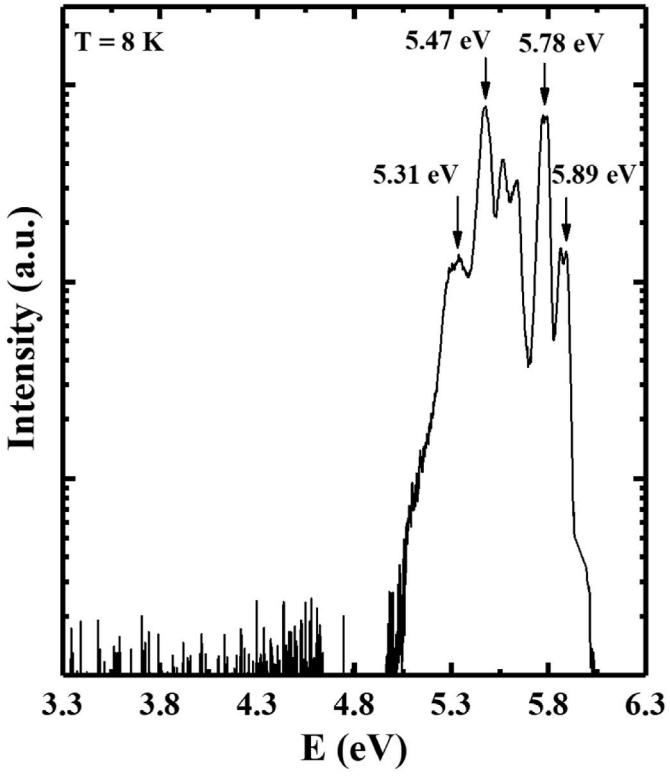

Fig. 1. Low temperature (8 K) PL spectra of pristine h-BN single crystal grown by the Ni–Cr flux method.

3. Results and discussions

Fig. 1 shows the low temperature (8 K) PL spectrum from a pristine flake of h-BN single crystal sample before annealing. The PL signal was recorded in the range from 3.3 to 6.3 eV. The PL spectrum shows the strong band edge emissions at 5.78 and 5.89 eV which are due to the optical and acoustic phonon assisted band edge transitions, respectively [3]. These peaks also show doublet peaks separated by a few meV due to the phonons. The optical and acoustic phonon energies of h-BN in the middle of the Brillouin zone are calculated for LO, TO, LA, and ZA as 200, 162, 83, 65 and 22 meV respectively [26]. The PL spectrum also shows a strong emission peak at 5.47 and additional multiple emission peaks between 5.30 and 5.78 eV. The origin of these emission peaks is believed to be due to stacking faults [27]. Cassabois et al. [28], also showed that these emissions peaks contain transverse optical phonon replicas due to intervalley scattering caused by stacking faults in h-BN. The PL signal of this sample below 5

eV is less than the noise level. In the PL spectrum of h-BN, frequently there is a broad emission band below 5 eV with peaks around 3.7 eV and/or 4.3 eV [22,29]. Emissions in the low energy bands are normally related to impurities such as residual foreign elements or native defects present in the samples. We did not see such an impurity band in our samples showing high crystalline and optical quality of the material. Their high quality was also previously verified by their superior performance in graphene devices [30].

To investigate the effect of annealing on the optical properties, PL measurements were carried out after annealing the samples at different temperatures and times in ambient air. The same samples were successively annealed and their PL spectra measured. We first performed a controlled experiment by varying the annealing temperature keeping the same annealing time. Fig. 2 shows the low temperature PL spectra from a sample after successive annealing at temperatures of about 300, 500 and 700 °C for 60 min. For annealing temperatures of 300 and 500 °C the PL emission peaks are similar to the pristine h-BN (Fig. 1b). The noise signal below 5 eV, however, has increased with repeated annealing. After annealing at 700 °C, new sharp emission peaks appear at 4.09, 3.89 and 3.69 eV. This clearly shows that the new peaks are caused by the annealing above 700 °C. Similar PL emissions appeared in annealed h-BN powder samples [31]. The peak at 4.09 eV is the zero-phone line (ZPL), and 3.89 and 3.69 eV are 1LO and 2LO phonon replicas of the ZPL, respectively. The longitudinal optical (LO) phonon in h-BN is 200 meV [26].

To optimize the conditions to generate the sharp emission at 4.09 eV, we further investigated the effects of the annealing temperature and time. Three h-BN flakes from same batch were annealed at temperatures of 800, 900 and 1000 °C, respectively for 20 min in ambient air. Low temperature PL measurements were performed for all those samples. These samples were again annealed successively at different times for 40 and 60 min keeping the same annealing temperature. Low temperature PL was measured after each successive annealing. Fig. 3 shows the PL spectra of the samples annealed at (a) 800, (b) 900, and (c) 1000 °C for different annealing time of 20, 40 and 60 min. For the sample annealed at 800 °C, a longer time is required to enhance the 4.09 eV peak with its phonon replicas. For the sample annealed at 900 °C for 60 min also has pronounced 4.09 eV emission. However, the sample annealed at 1000 °C shows the opposite behavior, the peaks are present for annealing time of 20 min but they disappeared after annealing for 40 and 60 min. For all conditions, band edge signals are not changed significantly. The noise signal below 5 eV, however, increases with repeated annealing as in Fig. 2 and increased annealing time for all these samples. We conclude that the 4.09 eV emission line can be generated by annealing the h-BN sample in the temperature range of 700–1000 °C, and lower annealing temperature requires longer annealing time and higher annealing temperature needs shorter annealing time. Thus, the optimized condition has window of annealing temperature in 700–950 °C for the duration of about 60 min to generate the 4.09 eV line.

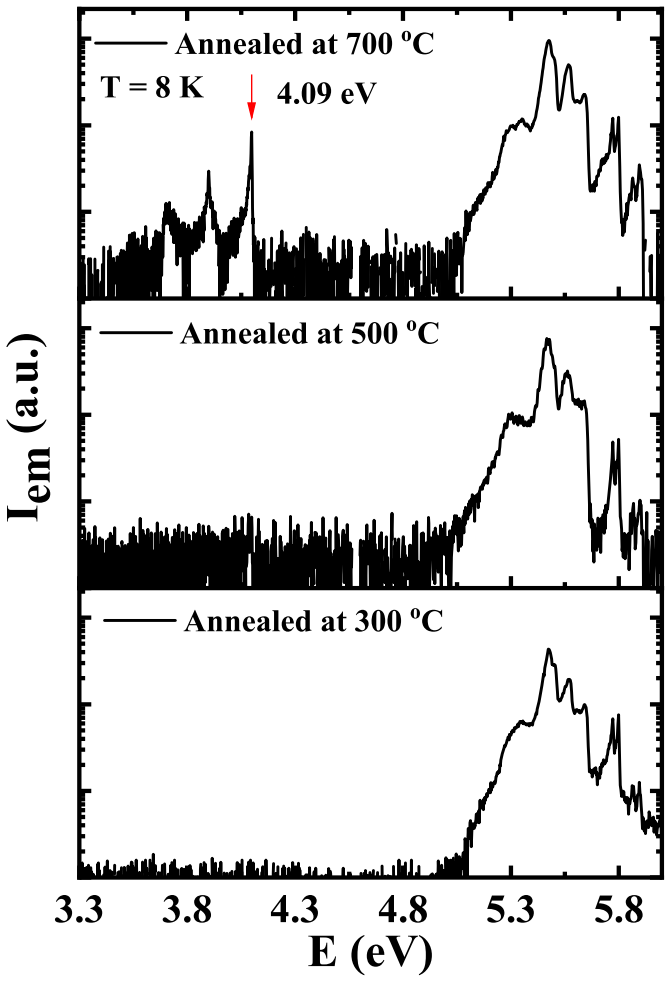

Fig. 2. PL spectra of an h-BN sample after successive annealing at different temperatures for 60 min.

To understand the nature of the sharp emission line at 4.09 eV and its electronic transition, we measured the PL while varying the temperature and laser power. Samples were prepared by annealing at 950 °C for 60 min in ambient air. Fig. 4a shows the PL spectra measured over the range from 3.5 to 4.5 eV by varying the temperature of the sample from 8 to 200 K. The intensities of the 4.1 eV emission line and phonon replicas decreased with increasing the temperature, most likely due to the thermal quenching via non-radiative channels. The sharp emission peak starts broadening above 80 K and the line width of the emission increased with increasing temperature. However, the peak position is almost indpendent of the temperature of sample. Fig. 4b shows the PL spectra by varying the average power of the excitation laser from 1 to 2 mW. The ZPL is well-resolved at 4.09 eV with LO phonon lines at 3.89 and 3.69 eV. There are also small shoulders at 3.91 and 3.71 eV which are about 20 meV above the 1LO and 2LO lines respectively, and could also be phonon related peaks. The intensity of the emission peak at 4.09 eV and its replicas increased with increasing excitation power due to increased carrier density. The intensity of the 4.09 eV emission line increased around 7 times as the excitation power is doubled from 1 to 2 mW. The line-width of the 4.09 eV peak for the highest excitation is about 0.2 nm (~3 meV). The sharp emission with line-width less than 1 nm clearly shows that it is an atomic-like emission. Despite the limited variation of excitation intensity, there was no sign of the shift of peak positions with increasing excitation power. From the PL intensity (I) in Fig. 4b, we estimated Huang-Rhys parameter, or S factor to be ~0.3 using the equation, $I = e^{-S}.S^n/n!$. The S factor value is the measure of electron-phonon coupling during optical transitions and the value obtained indicates weak electron phonon coupling [32].

Our results from the power and temperature dependent PL measurements show the emission peak position is stable. Single photon emission in the orange line (1.998 eV) in h-BN was also temperature independent [33]. Stable peak position in the PL measurements also indicates that the electronic transition involved in these emission process is less likely a donor and accepter pair (DAP) type. In the DAP transition the peak position is blue shifted due to the increased Coulomb interaction with increased DAP pairs caused by the excitation with high intensity of light [34].

The PL signal is mainly from the surface region of the samples as the penetration depth is less than micron. To understand if the annealing has affected the surface region or in the bulk of the material, in reference to the generation of the 4.09 eV line, the sample with the 4.09 eV was sputtered by Ar^+ ions to remove a few layers of the h-BN surface. We performed the low temperature PL measurement of the sample after sputtering by Ar^+ ions and shown in Fig. 5a. The PL signal is drastically changed with significantly reduced intensity in the band edge at 5.78 eV, and the sharp emission line at 4.09 eV completely disappears. However,

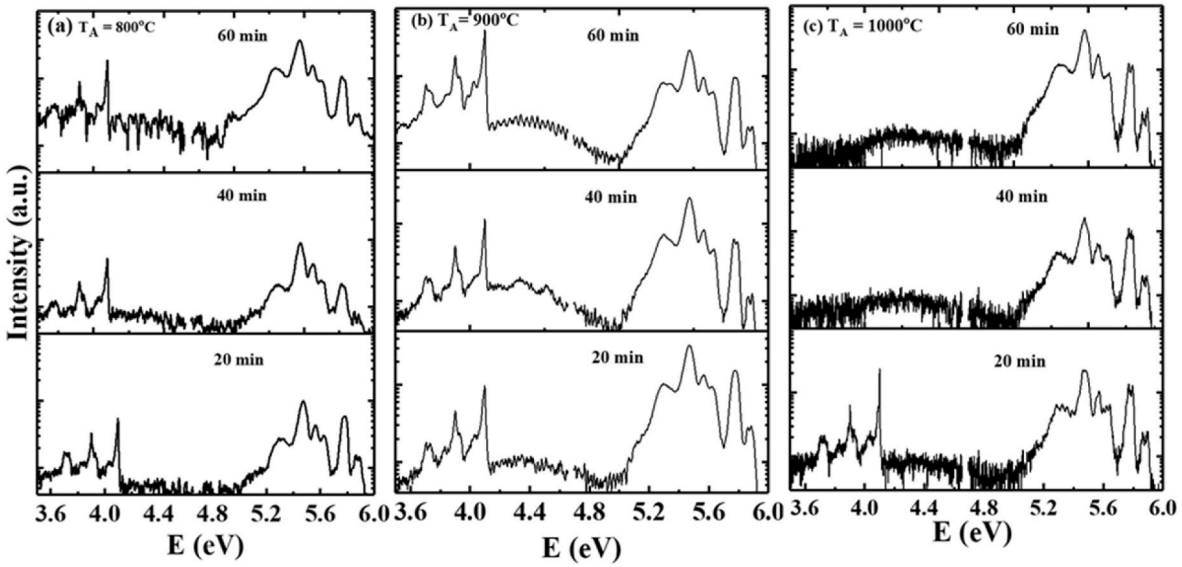

Fig. 3. Low temperature (8 K) PL spectra of bulk h-BN annealed at temperature (a) 800 °C, (b) 900 °C and (c) 1000 °C for different time of 20, 40 and 60 min.

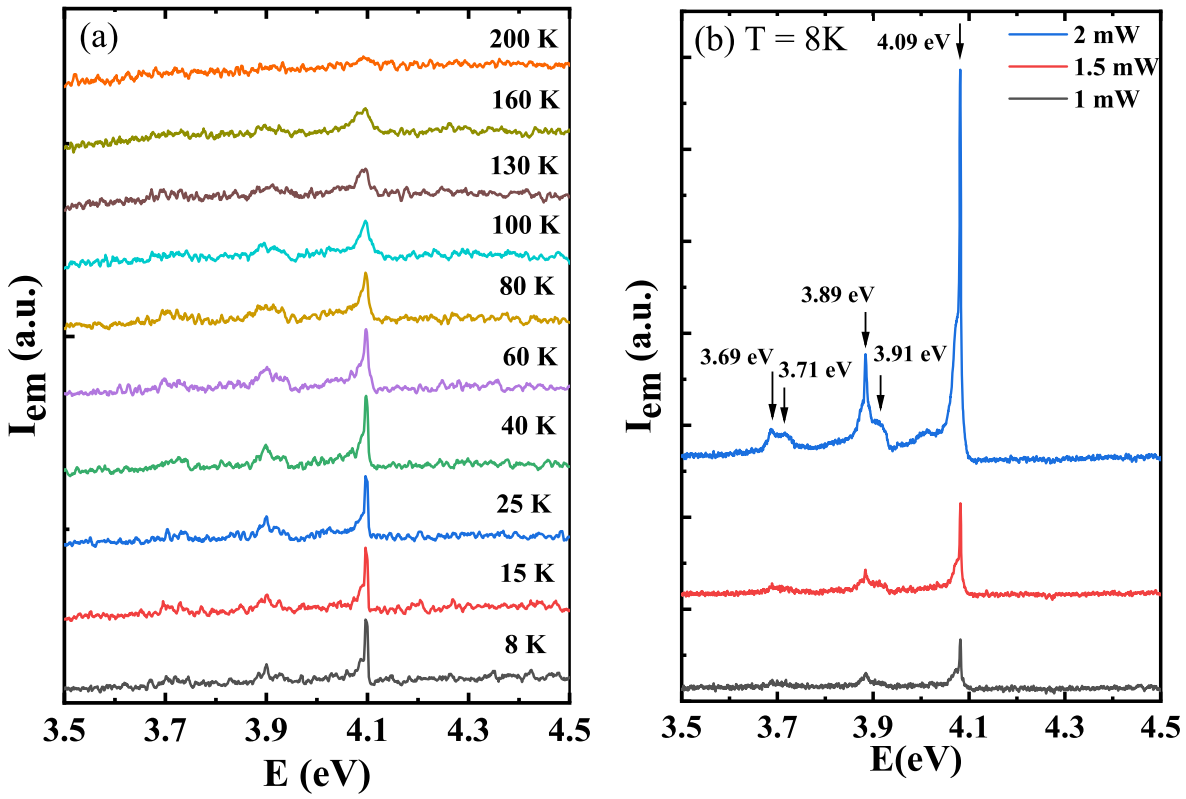

Fig. 4. (a) Temperature dependent PL spectra of h-BN sample measured by varying the sample temperature from 8 to 200 K, (b) Excitation power dependent PL spectra of h-BN sample measured at 8 K by varying excitation laser power from 1 to 2 mW.linewidth.

the spectrum has a broad impurity band with peak around 4.38 eV which could be caused by defects introduced by the Ar^+ sputtering. The decrease in the band edge intensity also indicates the surface structure damage by sputtering. Because of its layered crystal structure, the optical properties of h-BN are sensitive to its surface structure. Since the 4.09 eV line disappeared after sputtering, we conclude that the point defect responsible for this emission line could be residing in the surface region which was cleaned or damaged by the sputtering. Since the 4.09 eV emission line was generated by annealing as discussed above, we hypothesized that it can be recovered by reannealing. Fig. 5b shows the PL spectrum of the same sample after annealing again at 800 °C for 60 min. Interestingly, the sharp emission line at 4.09 eV reappeared along with its phonon replicas. Here, the emission line at 4.09 eV and its phonon replicas are superimposed with the broad impurity band peak around 4.38 eV. This further confirms that the atomic-like emission line at 4.09 eV is caused by annealing above 700 °C and indicates that the defect responsible for the emission line resides in the surface region. The PL spectrum after annealing also shows the significant enhancement of the band edge emission intensity. Annealing could repair the damage caused by argon sputtering. Lee et al. [35], reported improved structural and optical properties of h-BN thin films by annealing in nitrogen.

The sharp emission line at 4.09 eV and its phonon replicas were first reported by Bourrellier et al. [19], as single photon emission from defect points from a bulk h-BN using cathodoluminescence and commony known as 4.1 eV line in the literature. The 4.09 eV emission line observed in the PL with line-width less than 1 nm shows that it is an atomic-like emission due to the transition of electrons in highly localized states. The emission feature, and the peak positions of the ZPL and phonon replicas in our PL spectrum are at the same position as observed in the CL emission in that report. It suggests that the defect related to the origin of the emission lines is the same. Furthermore, the PL spectra were collected from a bulk sample with spot size of ~1 mm contrary to the emission from a defect site which about 80 nm. This suggests that the point defects responsible for this transition are abundant in the sample. This is important for practical device applications using bulk h-BN crystals. Bourrellier et al. [19], attributed the 4.09 eV line as a ZPL due to carbon impurity substitutional at the nitrogen site (C_N). Based on the PL study of h-BN micropowder in a wide temperature range from 7 to 1100 K, a model of (O_N–C_N)-complex was proposed as the origin of this line [36]. Chichibu et al. [37], assigned it to originate from C_N or V_BO_N in the spatio-time-resolved luminescence study of h-BN microcrystals. Although, several theoretical studies have been reported on the origin of the 4.1 eV line, the chemical structure of the defect responsible for the emission is still in debate. Most of the theoretical calculations suggest that the potential candidates for the defects responsible for the generation of the 4.1 emission line are carbon related. Different carbon related defect structures such as carbon dimer (C_BC_N), carbon ring (C6), $C_{4\ cis}$, and $C_{4\ trans}$ [38–42]. In a calculation, Hamdi et al. [43], proposed pentagon-hexagon Stone-Wales defect in h-BN for this emission. Further study and calculation are required to identify the chemical structure of the defect responsible for the 4.1 eV line and for its practical applications. Our experimental results of the emission line with spectrum feature without impurity band could be useful for theoretical calculation of the defects energies. Further experiments are also underway to identify the defect by comparing the samples with and without the 4.09 eV emission line.

4. Conclusions

In summary, we characterized the flakes of h-BN single crystal grown by Ni–Cr flux method for optical properties using a deep UV PL spectroscopy and studied the effect of thermal annealing. Thermal annealing in ambient air produced an atomic-like emission in UV region at 4.09 eV. The 4.09 eV emission line was generated by annealing h-BN samples in the temperature range of 700–950 °C for about 60 min in ambient air. Our study also indicates the defect responsible for the emission line

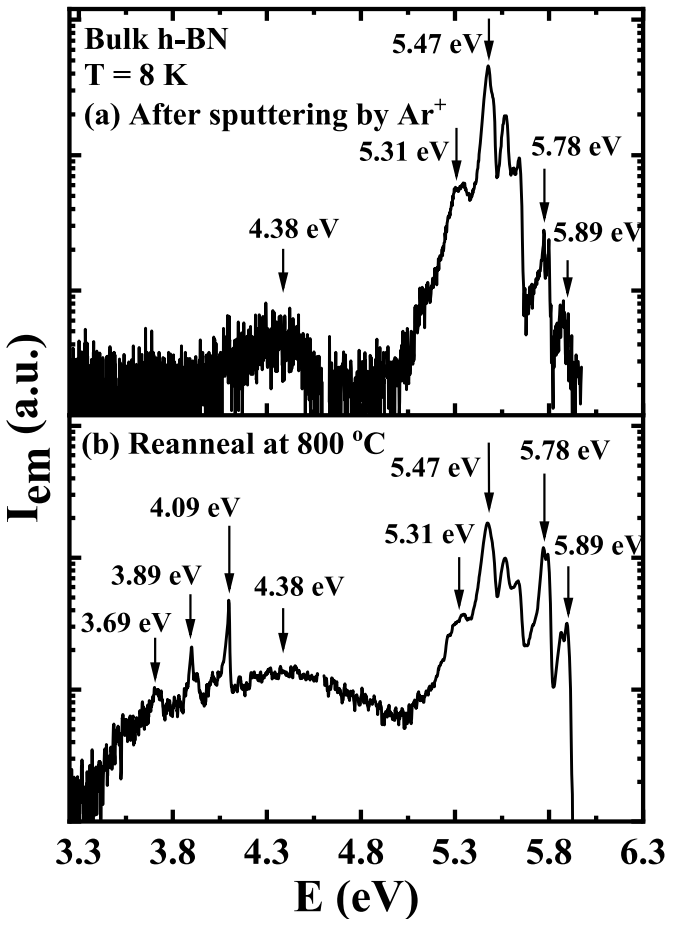

Fig. 5. PL spectra of annealed h-BN sample (a) after sputtering by argon ion and (b) reannealing at 800 °C for 60 min.

resides on the surface region. The energy peak of the atomic-like emission line at 4.09 eV was stable based on the temperature and power dependent PL measurements.

CRediT authorship contribution statement

N. Maharjan: Writing – original draft, Validation, Methodology, Investigation, Formal analysis. **P. Joshi:** Writing – review & editing, Methodology, Conceptualization. **E. Janzen:** Methodology, Investigation. **J.H. Edgar:** Writing – review & editing, Supervision, Funding acquisition, Conceptualization. **N. Khan:** Writing – review & editing, Validation, Methodology, Conceptualization. **M.L. Nakarmi:** Writing – review & editing, Supervision, Project administration, Funding acquisition, Conceptualization.

Declaration of competing interest

The authors declare that they have no known competing financial interests or personal relationships that could have appeared to influence the work reported in this paper.

Data availability

Data will be made available on request.

Acknowledgements

We acknowledge the support from National Science Foundation (NSF) USA grant (DMR – 2117286), ASRC seed grant, PSC-CUNY grant and Grace Spruch Physics'47 grant at Brooklyn College for this study. Support for the h-BN crystal growth from the Office of Naval Research, USA award N00014-20-1-2427 is greatly appreciated.

References

[1] D.A. Lenonis, Boron nitride powder: a review, ceramic technology international, Sterling Publ. (1994) 57–61.
[2] K. Watanabe, K. Taniguchi, H. Kanda, Nat. Mater. 3 (2004) 404.
[3] G. Cassabois, P. Valvin, B. Gil, Nat. Photonics 10 (2016) 262.
[4] A. Bergh, G. Craford, A. Duggal, R. Haitz, "The promise and challenge of solid-state lighting", Physics Today 54, December 42 (2001).
[5] A. Khan, K. Balakrishnan, T. Katona, Nat. Photonics 2 (2008) 77.
[6] K. Watanabe, T. Taniguchi, T. Niiyama, K. Miya, M. Taniguchi, Nat. Photonics 3 (2009) 591.
[7] K. Watanabe, T. Taniguchi, H. Kanda, Phys. Stat. Sol (a) 201 (2004) 2561–2565.
[8] J. Li, R. Dahal, S. Majety, J.Y. Lin, H.X. Jiang, Nuclear inst, Methods in Physics Research A 654 (2011) 417.
[9] J.D. Caldwell, I. Aharonovich, G. Cassabois, J.H. Edgar, G. Bernard, D.N. Basov, Nat. Rev. Mater. 4 (2019) 552–567.
[10] C.R. Dean, A.F. Young, I. Meric, C. Lee, L. Wang, S. Sorgenfrei, K. Watanabe, T. Taniguchi, P. Kim, K.L. Shepard, J. Hone, Nat. Nanotechnol. 5 (2010) 722.
[11] J. Xue, J.S. Yamagishi, D. Bulmash, P. Jacquod, A. Deshpande, K. Watanabe, T. Taniguchi, P.J. Herrero, B.J. LeRoy, Nat. Mater. 10 (2011) 282.
[12] I. Aharonovich, D. Englund, M. Toth, Nat. Photonics 10 (2016) 631.
[13] T.T. Tran, C. Elbadawi, D. Totonjian, C.J. Lobo, G. Grosso, H. Moon, D.R. Englund, M.J. Ford, I. Aharonovich, M. Toth, ACS Nano 10 (2016) 7331–7338.
[14] N.R. Jungwirth, B. Calderon, Y. Ji, M.G. Spencer, M.E. Flatté, G.D. Fuchs, Nano Lett. 16 (2016) 6052.
[15] N. Mendelson, D. Chugh, J.R. Reimers, et al., Nat. Mater. 20 (2021) 321–328.
[16] A. Hernández-Mínguez, J. Lähnemann, S. Nakhaie, J.M.J. Lopes, P.V. Santos, Phys. Rev. Appl. 10 (2018), 044031.
[17] F. Hayee, L. Yu, J.L. Zhang, C.J. Ciccarino, M. Nguyen, A.F. Marshall, I. Aharonovich, J. Vučković, P. Narang, T.F. Heinz, J.A. Dionne, Nat. Mater. 19 (2020) 534–539.
[18] M. Koperski, K. Pakuła, K. Nogajewski, A.K. Dąbrowska, M. Tokarczyk, T. Pelini, J. Binder, T. Fąs, J. Suffczyński, R. Stępniewski, A. Wysmołek, M. Potemski, Sci. Rep. 11 (2021) 15506.
[19] R. Bourrellier, S. Meuret, A. Tararan, O. Stéphan, M. Kociak, L.H. Tizei, A. Zobelli, Nano Lett. 16 (2016) 4317.
[20] M.G. Silly, P. Jaffrennou, J. Barjon, J.-S. Lauret, F. Ducastelle, A. Loiseau, E. Obraztsova, B. Attal-Tretout, E. Rosencher, Phys. Rev. B 75 (85205) (2007).
[21] L. Schué, I. Stenger, F. Fossard, A. Loiseau, J. Barjon, 2D Mater. 4 (2017), 015028.
[22] T.Q.P. Vuong, G. Cassabois, P. Valvin, A. Ouerghi, Y. Chassagneux, C. Voisin and, B. Gil, phys. Rev. Lett. 117 (2016) 97402.
[23] L. Museur, E. Feldbach, A. Kanaev, Phys. Rev. B 78 (2008) 155204.
[24] T.B. Hoffman, B. Clubine, Y. Zhang, K. Snow, J.H. Edgar, J. Cryst. Growth 393 (2014) 114.
[25] T.B. Hoffman, Y. Zhang, J.H. Edgar, N. Khan, R. Szoszkiewicz, Mater. Sci. Technol. 1591 (2014).
[26] J. Serrano, A. Bosak, R. Arenal, M. Krisch, K. Watanabe, T. Taniguchi, H. Kanda, A. Rubio, L. Wirtz, Phys. Rev. Lett. 95503 (98) (2007).
[27] R. Bourrellier, M. Amato, L.H. Galvão, Tizei, C. Giorgetti, A. Gloter, M.I. Heggie, K. March, O. Stephan, L. Reining, M. Kociak, A. Zobelli, ACS Photonics 1 (2014) 857.
[28] G. Cassabois, P. Valvin, B. Gil, Phys. Rev. B 93 (35207) (2016).
[29] L. Museur, E. Feldbach, A. Kanaev, Phys. Rev. B 78 (2008) 155204.
[30] J. Sonntag, J. Li, A. Plaud, A. Loiseau, J. Barjon, J.H. Edgar, C. Stampfer, 2D Mater. 31009 (7) (2020).
[31] N. Maharjan, P. Joshi, R.C. Rai, M.L. Nakarmi, J. Lumin. 234 (2021) 117944.
[32] I. Pelant, J. Valenta, Luminescence Spectroscopy of Semiconductors, Oxford University Press, New York, 2012.
[33] M. Koperski, K. Nogajewski, M. Potemski, Opt Commun. 411 (2018) 158.
[34] J.I. Pankove, Optical Processes in Semiconductors, Dover Publications Inc., New York, 1971.
[35] S.H. Lee, H. Jeong, O. Francis, N. Okello, S. Xiao, S. Moon, D.Y. Kim, G.-Y. Kim, J.-I. Lo, Y.-C. Peng, B.-M. Cheng, H. Miyake, S.-Y. Choi, J.K. Kim, Sci. Rep. 9 (2019) 10590.
[36] A.S. Vokhmintsev, I.A. Weinstein, J. Lumin. 230 (2021) 117623.
[37] S.F. Chichibu, Y. Ishikawa, H. Kominami, K. Hara, J. Appl. Phys. 123 (65104) (2018).
[38] M. Mackoit-Sinkevičienė, M. Maciaszek, C.G. Van de Walle, A. Alkauskas, Appl. Phys. Lett. 115 (2019) 212101.
[39] C. Linderälv, W. Wieczorek, P. Erhart, Phys. Rev. B 103 (2021) 115421.
[40] T. Korona, M. Chojecki, Int. J. Quant. Chem. 119 (2019), 25925.
[41] S. Li, A. Pershin, G. Thiering, P. Udvarhelyi, A. Gali, J. Phys. Chem. Lett. 13 (2022) 3150.
[42] S. Li, A. Pershin, P. Li, A. Gali, npj 2D Mater Appl 8 (2024) 16.
[43] H. Hamdi, G. Thiering, Z. Bodrog, V. Ivády, A. Gali, npj Comput. Mater. 6 (2020) 178.